Materials Science Forum
ISSN: 1662-9752, Vol. 1182, pp 125-134
doi:10.4028/p-2Og3qz

Submitted: 2026-01-14
Revised: 2026-02-13
Accepted: 2026-02-20
Online: 2026-04-10

Simulation and Experimental Investigation of the LRI Process for Particle-Filled Resins in Aerostructure Applications

Nihad Siddig[1,a*], Mohamed Mtibaa[1,b] and Marie Coupé[1,c], Alexandre Guinoiseau[1,d]

[1]Nantes Université, IRT Jules Verne, 1 Mail des 20 000 Lieues, 44340 Bouguenais, France

[a*]nihad.siddig@irt-jules-verne.fr, [b]mohamed.mtibaa@irt-jules-verne.fr, [c]marie.coupe@irt-jules-verne.fr, [d]alexandre.guinoiseau@irt-jules-verne.fr

Keywords: Composites, Liquid Resin Infusion (LRI), Simulation, Particle-filled Resins

Abstract. This work primarily focuses on the development and simulation of the Liquid Resin Infusion (LRI) process for particle-filled resins, aiming to impart additional functionalities to composite parts. The paper presents both the simulation development and the experimental tests used to establish physics-based models. The main challenge lies in understanding how particle addition affects the resin flow process. The introduction of particles increases resin viscosity, which in turn influences flow behaviour. Moreover, particle filtration by the fibrous medium changes its permeability, thereby impacting both flow dynamics and particle distribution. The materials used in the infusion process are experimentally characterised, and the resulting parameters served as inputs for the LRI process simulations. Constitutive behavior laws are implemented within the simulation tool. Simulations are then conducted using all characterized inputs and models for validation purposes. These validated models are subsequently employed to assess the infusion process performance.

Introduction

The European project PAIRAMID aims to transform the design, development, and certification of aerostructures through an AI-driven digital framework that integrates virtual testing at every level of the certification pyramid, from material to coupon, element, and full aerostructure (Figure 1). By leveraging advanced simulations and data-driven insights, this approach reduces the reliance on costly and time-consuming physical tests, enabling a more efficient and integrated certification process. The project focuses on the fabrication of aeronautical parts using two manufacturing processes: Liquid Resin Infusion (LRI) and Fused Deposition Modelling (FDM). This paper concentrates on the former. The LRI process in the PAIRAMID project includes adding particles to improve the electrical conductivity of composite components, such as the wing front edge and the aerostructure door skin. This functionality is essential for applications such as lightning strike protection and electrostatic discharge mitigation, allowing for the integration of electrical performance directly into the composite structure. Model particles are used herein to investigate the particle-filled LRI process.

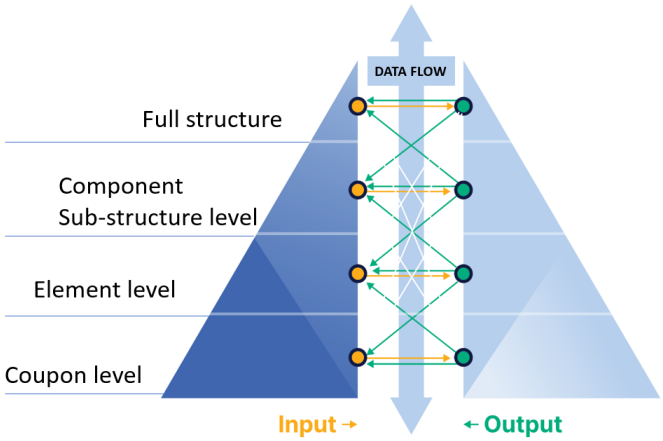

Fig. 1. The pAIramid project approach

Context of the study

This study focuses on developing and simulating the Liquid Resin Infusion (LRI) process [1] for particle-filled resins. The paper details both the simulation framework and the experimental work carried out to build physics-based models [2-4]. The materials involved in the infusion process are experimentally characterized. Simulations based on all characterized inputs and models are then performed and compared to infusion experiments with particle-filled resins [5-9].

Experimental Method

The project investigates the infusion process with particle-filled resin with different particle sizes and percentages. The different percentages are tested to evaluate their influence on the process and to verify if the model can predict the process behaviour in the presence of these particles.

Material characterization

The main materials used for the infusion trials are unidirectional glass fibre reinforcements from Owens Corning, fibre diameter of about 17 µm, oriented at the flow direction for all the experiments. The epoxy resin Infugreen SR 8100/SD 8822 is used for the fabrication of composites. The ATH particles M15B and M20B from LKAB, with three concentrations (10%, 15% and 20%), respectively, were added to study the influence on the process. The particles are rigid and polydisperse with narrow distribution, where the vast majority of particles are on the order of 15 µm for M15B and 20 µm for M20B, respectively. They are characterized as non-deformable. Figure 2 shows a microscopic observation of the fabricated composite, functionalised with the grade M20B, showing particles, fibre bundles and stitching.

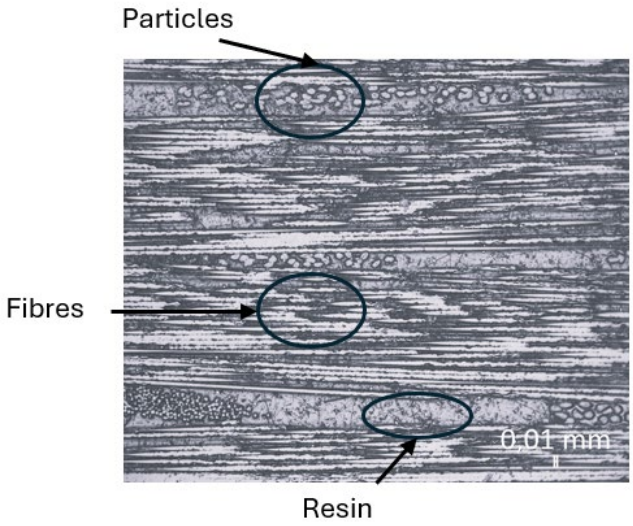

Fig. 2. Microscope observation of the composite

The viscosity of neat resin was measured by Sicomin. The permeability of the reinforcements was measured by TENSYL in the in-plane and out-of-plane directions and the values are used as input for simulations. The permeabilities and viscosities will be modified by particle addition. Previous studies have shown the influence of particles on both resin and fabric [6-9]. The variation in permeability during infiltration is modelled (by Eqs. 7 and 8) as being a result of particle filtration and clogging of the fibrous medium. A key assumption revolves around the fact that the rigid particles do not mechanically compress or permanently displace the fibre preform. While the particles modify the permeability of the medium and are intended to impart functional properties (e.g., electrical conductivity) to the final composite, they may modify the architecture of the fibrous medium but not the individual glass fibres.

Process conditions

The process is pressure-controlled, as governed by Darcy's law (Eq. 2). The resin enters the part at atmospheric pressure (on the left of Figure 3), and vacuum pressure is applied and controlled at the resin outlet (on the right of Figure 3). A pressure gradient of 0.8 bar is driving the flow. The extended infusion time is a direct consequence of this low driving pressure gradient combined with the significant increase in suspension viscosity and the progressive reduction in reinforcement permeability due to particle filtration, as described by the constitutive models in Section 4.

Infusion tests

Several infusion trials are conducted to improve the understanding of the process and to provide input parameters for the process simulation [6]. The infusion trials are illustrated in Figure 3 for three different configurations, with a stacking of 7 plies of unidirectional reinforcement having the same in-plane dimensions as illustrated by the figure, giving a thickness of about 4mm, and a fibre volume fraction of approximately 50%.

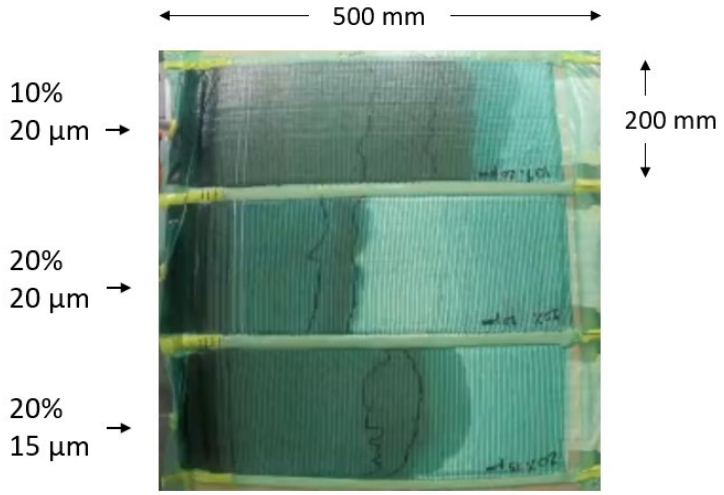

Fig. 3. Infusion trials with different particle sizes and percentages

Figure 3 presents three infusion trials carried out simultaneously under identical process conditions, using two particle sizes (15 µm and 20 µm) and two particle concentrations (10% and 20%), observed 1 h after the start of the infusion. The figure shows that the lowest particle concentration resulted in the most successful infusion among the tested cases. At a given concentration, particle size governs the infusion behaviour, as the 15 µm case exhibited a more advanced flow front than the 20 µm case at the same instant of time.

Modelling and simulation

To simulate the flow of a particle-filled resin through a porous medium, it is necessary to adopt physical models capable of representing the main phenomena involved, in particular, fluid flow, the filtration of particles within the reinforcement [7]. This simulation is based on the coupling of two fundamental models:

- The fluid flow in the fibrous medium model
- The particle filtration model
- The suspension concentration evolution model
- Material behaviour laws (permeability and viscosity)

On the one hand, filtration leads to changes in the local particle concentration, partial retention of these fillers within the fibrous reinforcement, and progressive modifications of the porosity and permeability of the medium. On the other hand, the resin flow is directly influenced by these changes, in particular the reduction in permeability due to progressive clogging (particle accumulation) and variations in viscosity, which itself depends on the local particle concentration [8].

The flow is governed by the continuity equation (Eq. 1) and Darcy's law (Eq. 2).

$$\nabla \cdot \vec{U} = 0 \tag{1}$$

where $\vec{U}$ is the velocity vector.

$$\vec{U} = -\frac{\boldsymbol{K}}{\mu}\nabla p \tag{2}$$

where $\boldsymbol{K}$ is the permeability tensor, μ is the viscosity and ∇p is the pressure gradient.

The porosity ε of the fibrous medium is described by equation (Eq. 3). It represents the change in porosity as a result of particle retention.

$$\varepsilon = \varepsilon_0 - \sigma \tag{3}$$

where ε_0 is the initial porosity and σ is the retention, which is governed by the equation (Eq. 4).

$$\frac{\partial \sigma}{\partial t} = \alpha \vec{U} C \left(1 - \frac{\sigma}{\sigma_u}\right) \quad (4)$$

where α is the filtration coefficient, a measure of the medium's efficiency at capturing particles, with m^{-1} unit, C is the concentration, and σ_u is the ultimate particle deposit at which the clogging of the porous medium occurs, representing the maximum particle retention capacity of the porous medium. It is the value of σ at which the retention rate $\frac{\partial \sigma}{\partial t}$ becomes zero [6,8]. The equation considers that the retention rate is proportional to the flux of suspended particles, represented by the term $\vec{U}C$. The proportionality constant is called the filtration coefficient α. This coefficient represents the probability of particle capture; it depends on its initial value α_0, the porosity and the permeability. The filtration coefficient changes according to this relation (Eq. 5).

$$\alpha = \alpha_0 \left[\left(\frac{K}{K_0}\right)^{-\frac{1}{2}} \left(\frac{\varepsilon}{\varepsilon_0}\right)^{\frac{3}{2}} \left(\frac{1-\varepsilon}{1-\varepsilon_0}\right)^{-1} \right]^{a_1} \quad (5)$$

where K_0 is the initial permeability and a_1 is an empirical positive constant [7, 8].

The concentration is governed by this conservation equation (Eq. 6) [6, 8]. This equation is the resulting mass balance after applying mass conservation on the three species involved: the fluid, the retained and suspended particles.

$$\frac{\partial [\varepsilon C]}{\partial t} + \nabla \cdot \{\vec{U} C\} + \frac{\partial \sigma}{\partial t} = 0 \quad (6)$$

The change in medium permeability K is governed by the electrical analogy equation, Eq. 7, applied to the initial filter permeability K_0 and the deposit permeability K_d [6].

$$K = \frac{K_0 . K_d}{K_0 + K_d} \quad (7)$$

The deposit permeability K_d is estimated by the Kozeny-Carman relation given in Eq. 8.

$$K_d = \frac{d^2 (1-\sigma)^3}{36 h_K \sigma^2} \quad (8)$$

where d is the particle diameter and h_K is the Kozeny constant (Eq. 8).

The viscosity is modelled by equation 9. This model was proposed by Erdal [7], and it assumes that the viscosity depends uniquely on the particle concentration. In this equation, the suspension is assumed to be Newtonian and the viscosity change occurs at a constant shear rate [8].

$$\mu = \mu_0 \left[1 - \frac{C}{A}\right]^{-2} \quad (9)$$

where A is the packing fraction.

Simulation

The simulation is realized by COMSOL Multiphysics to model the coupling of suspension flow and particle retention, leading to a coupling between the linear and non-linear equations presented in this section. The continuity equation (1), along with Darcy's law (2) are implemented in the tool to

compute the flow of suspensions. In addition, two user-defined partial differential equations (PDEs) are defined to model the filtration kinetics and the concentration conservation equations. A time-dependent study with Phase initialization is introduced to solve the problem [8]. The calculation loop is illustrated in Figure 4.

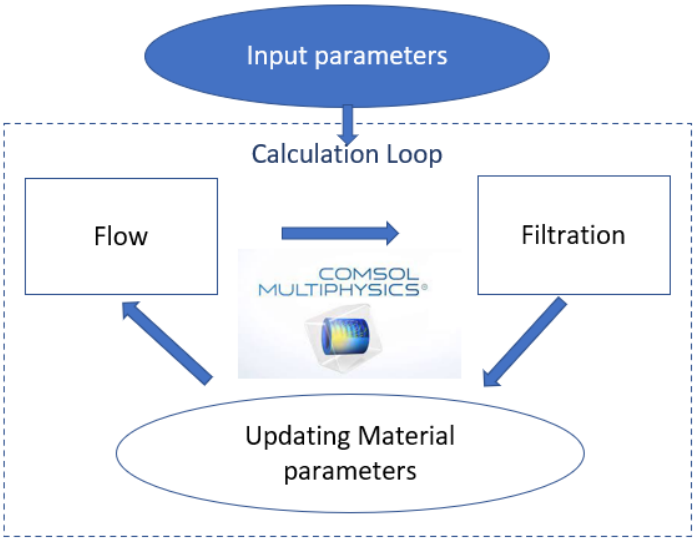

Fig. 4. Calculation loop in COMSOL Multiphysics

The model developed is used for simulating the suspension flow through the fibrous medium in LRI process. The initial conditions (at time $t = 0$), at any point of the preform, pressure $P(x, 0) = P_{Vacuum}$, retention $\sigma(x, 0) = 0$, porosity $\varepsilon(x, 0) = \varepsilon_0$ and particle concentration $C(x, 0) = 0$. For the boundary conditions, at the inlet $(x = 0)$, during infusion $P(x = 0, t) = P_0$, $C(x = 0, t) = C_0$, while at the front $\big(x = L(t)\big)$, $P(x = L(t), t) = P_{Vacuum}$ and $\sigma(x = L(t), t) = 0$.

The parameters used for this simulation are presented in Table 1.

Table 1. Parameters used in the models and their corresponding values

V_{f_0}: Fibers' volume fraction (%)	50%
α_0: Initial filtration coefficient (m^{-1})	1 [10]
P_0: Atmospheric pressure (Pa)	1.01325x10^5
P_{Vacuum} : Vacuum pressure (Pa)	0.2x10^5
σ_u: Ultimate specific deposit	0.5
A : Empirical constant	0.68 [10]
a_1 : Parameter model	1 [10]
L_0: Length (m)	0.5
L_1: Width (m)	0.2
H_0: Height (m)	0.004
μ_0: Initial viscosity (Pa. s)	Characterisation
K_0: Initial permeability (m^2)	Characterisation

Simulation results and correlation

The simulation model was first developed using pure resin, without including the filtration models, and then compared with the experimental results. Figure 5 presents the experimental and numerical flow front positions. The filling model shows good agreement with the experimental data.

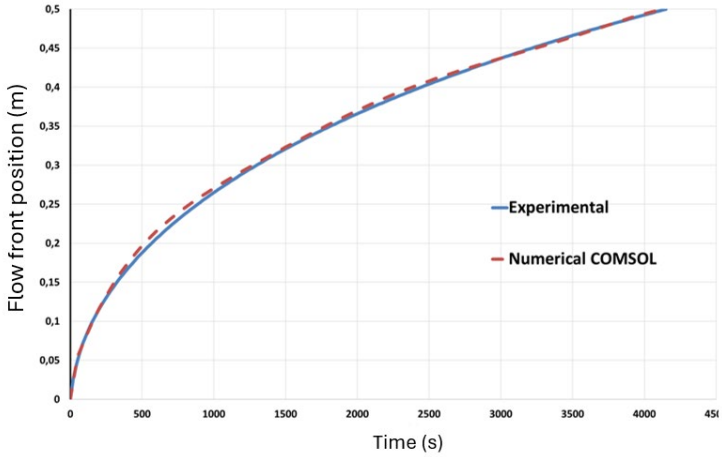

Fig. 5. Flow front advancement, comparison between experimental and numerical results with pure resin

Figure 4 presents the cases studied, both experimentally and numerically. Two different particle sizes were considered (15 µm and 20 µm). As described in Section 2, the numerical model incorporates particle size through its effect on deposit permeability. The images present the flow front position at 16 minutes from the beginning of the infusion for the experiments with 15 µm resin suspensions.

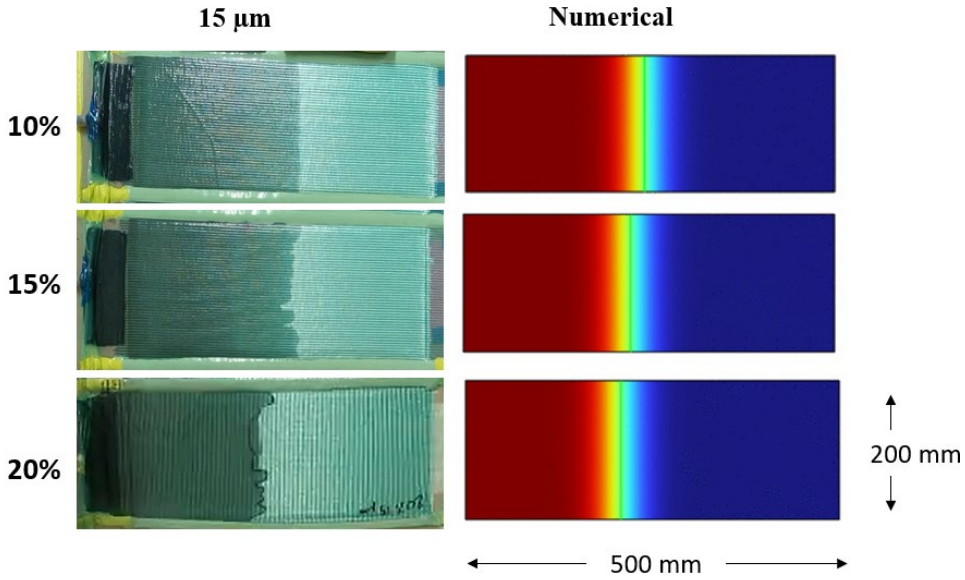

Fig.6. Correlations between numerical and experimental results with particle-filled resin

Figure 6 shows that the predictions provided by the simulation present deviations from experimental measurements. The figure shows that, numerically, the 10% suspension concentration advances further than the higher concentrations (15% and 20%). This can be explained by the increase in particle content at higher concentrations, which consequently increases viscosity and decreases permeability, thereby delaying the flow front. However, experimentally, the flow front positions for 10% and 15% are very close. This may result from process variability, the suspension preparation method, potential particle sedimentation and resin transfer to the part, all of which can introduce errors in the actual particle concentration [11].

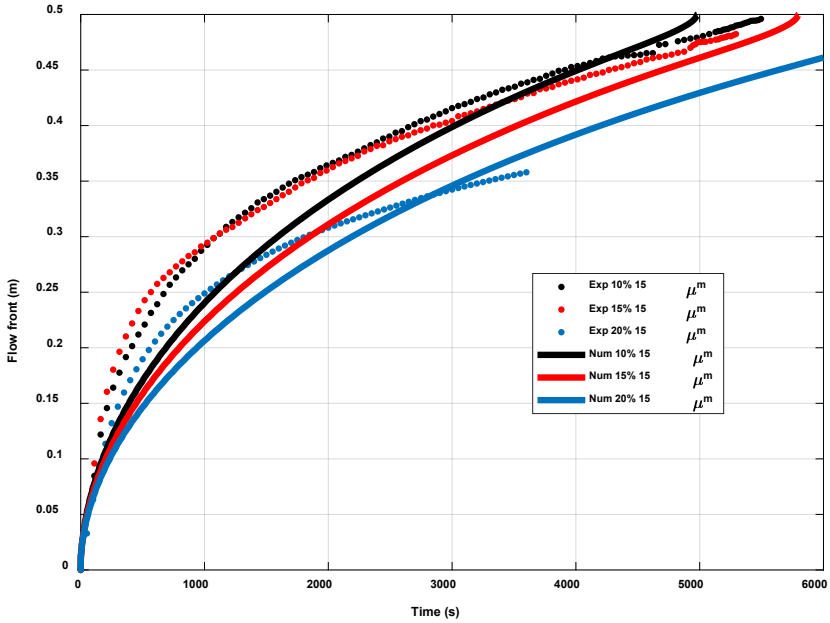

Fig. 7. Flow front advancement, comparison between experimental and numerical results with particle-filled resin

Figure 7 illustrates the comparison between numerical and experimental results for front advancement over time, considering three different initial particle concentrations (10%, 15%, and 20%) at the same particle size (15 µm). The results indicate a discrepancy between the numerical predictions and the experimental data, which is likely due to insufficient control of the initial particle concentration entering the part during the experimental tests because of potential sedimentation. Although the suspension is prepared with a nominal concentration of 20%, the effective concentration during infusion may differ and may either be higher or lower than the theoretical concentration. However, the numerical model could approximate the overall filling time for the 10% and 15% concentration cases, but the evolution of the flow front remains different from the experiment for all the concentrations. This observation supports the hypothesis that the effective concentration infused during the experimental tests may differ from the nominal concentration.

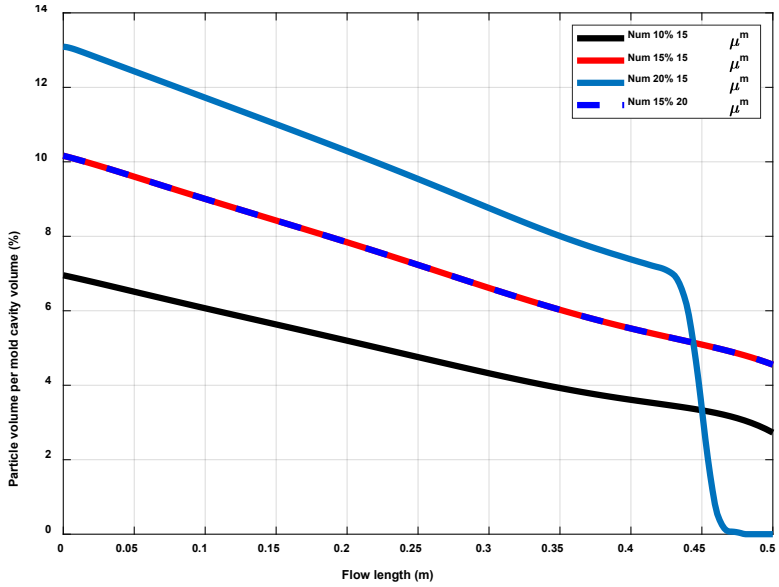

Fig. 8. The final particle distribution in the part

The particle quantity evolution along the length is shown in Figure 8. As expected, increasing the initial particle concentration leads to an increase in the particle quantity in the composite. In the case of a 20% concentration and 15 µm particle size, the selected maximum infusion time (6000 s) is not

sufficient to fill the part. As a result, the particle quantity drops to zero in the unfilled (dry) area. In addition, the influence of particle size on the evolution of the amount of particles in the composite was examined, and no significant effect was observed. This may be attributed to the model's limited ability to accurately represent particle-size-dependent filtration mechanisms. In the governing equations, the retention does not depend directly on permeability, but rather on the filtration coefficient, which itself is a function of permeability. However, the variation of α is very limited; therefore, the resulting difference is not significant, either in terms of retention or concentration.

Multiple criteria were tested to investigate the infusion limit of clogging. In Figure 9, the criterion developed by [6] is tested.

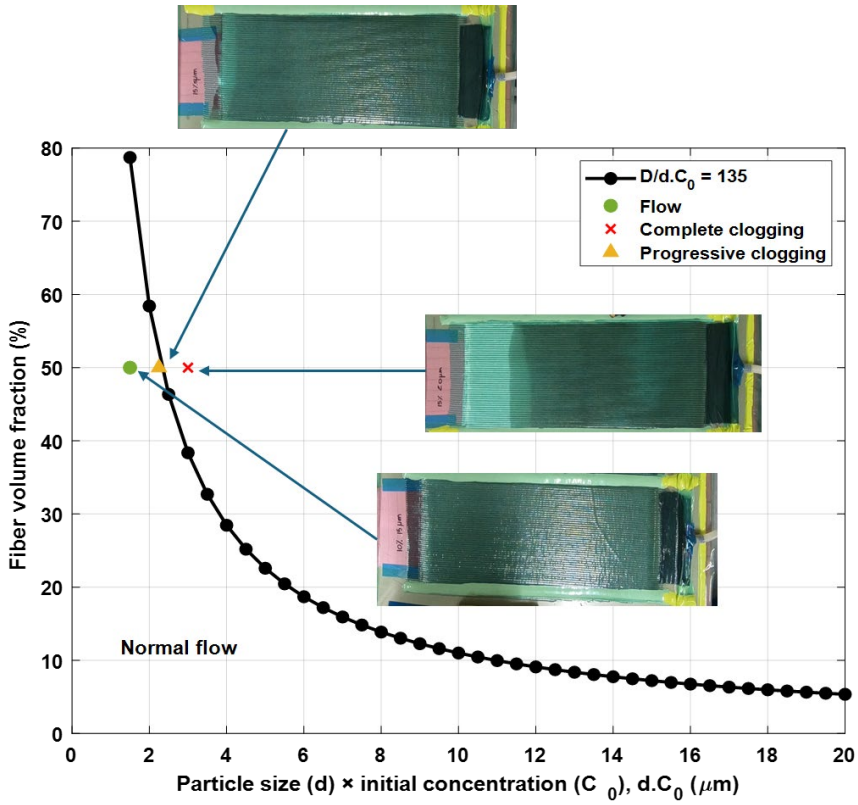

Fig.9. The clogging criterion

This clogging criterion allows for determining whether the part can be fully filled or whether clogging prevents complete impregnation (Figure 9). For the three experimental tests considered, the criterion was evaluated by multiplying the particle size ($d = 15\ \mu m$) by the initial particle concentration ($C_0 = 10\%, 15\%\ and\ 20\%$), with a fiber volume fraction of 50%. The results show that for an initial concentration of 10% and a particle size of 15 µm, the part can be filled experimentally. In contrast, for 15% and 15 µm, progressive clogging occurs, which is consistent with the experimental observations, as filling becomes increasingly difficult toward the end of the process. Finally, in the case of 20% and 15 µm, complete clogging is observed; experimentally, after a certain time, the particle-filled resin no longer advances.

Conclusion and Perspectives

The article presented the main models describing particle-filled resin infusion through fibrous media. Key results included LRI process infusion trials performed with different particle sizes and concentrations. Numerical simulation results were presented and correlated with experimental tests. The simulations showed good agreement with the experiments in terms of flow-front advancement and present a prediction of particle content; however, the models are not very sensitive to particle size and mainly depend on particle concentration. The models should be validated using CNT suspensions, with systematic correlation to experimental results. The performed infusion trials are

consistent with the clogging criterion. Future developments should focus on comparing experimental and numerical particle content and on predicting the LRI process for complex particle-filled components.

Acknowledgement

This project has received funding from the European Union's Horizon Europe research and innovation programme under grant agreement No 101192736.

References

[1] P. Le Bot, G. Lebreton, N. Siddig, P. Couarraze, O. Fouché, C. Sébastien, A. De Fontgalland, F. Cara, P. Gérard, Anomaly detection during thermoplastic composite infusion: Monitoring strategy through thermal sensors, Key Engineering Materials, 926 (2022), 1423–1436.

[2] P. Carlone, F. Rubino, V. Paradiso, F. Tucci, Multi-scale modeling and online monitoring of resin flow through dual-scale textiles in liquid composite molding processes, The International Journal of Advanced Manufacturing Technology, 96 (2018), 2215–2230.

[3] F. Rubino, P. Carlone, A semi-analytical model to predict infusion time and reinforcement thickness in VARTM and SCRIMP processes, Polymers (Basel), 11(1) (2018), 20, doi:10.3390/polym11010020.

[4] C. H. Park, Numerical simulation of flow processes in composites manufacturing, in Advances in Composites Manufacturing and Process Design, Woodhead Publishing, 2015, pp. 317–378, doi:10.1016/B978-1-78242-307-2.00015-4.

[5] H. Cherif, M. Mtibaa, A. Saouab, K. Essassi, A. El Hami, A. Bouguecha, M. Haddar, Numerical modeling of suspension impregnation in fibrous media: Application to the VARI process, Materials Research Express, 12(11) (2025), 115010.

[6] D. Lefevre, S. Comas-Cardona, C. Binétruy, P. Krawczak, Modelling the flow of particle-filled resin through a fibrous preform in liquid composite molding technologies, Composites Part A: Applied Science and Manufacturing, 38(10) (2007), 2154–2163.

[7] M. Erdal, S. I. Güçeri, S. C. Danforth, Impregnation molding of particle-filled preceramic polymers: Process modeling, Journal of the American Ceramic Society, 82(8) (1999), 2017–2028.

[8] N. A. Siddig, Experimental and numerical modeling of the impregnation of fibrous media by suspensions in LCM processes (Doctoral dissertation, Normandie Université, 2021).

[9] L. Marchand, S. Comas-Cardona, C. Binetruy, A. Hautefeuille, Caractérisation des matériaux pour RTM chargé dans des préformes fibreuses 3D, in Journées Nationales sur les Composites 2025, June 2025.

[10] M. Mtibaa, A. Saouab, A. E. Moumen, S. Bouaziz, A. E. Hami, M. Haddar, Contribution to manufacturing control of particle-filled composites by RTM process, The International Journal of Advanced Manufacturing Technology, 134(1) (2024), 75–95.

[11] N. A. Siddig, L. Bizet, A. El Moumen, A. Saouab, Experimental characterization of polydisperse particle-loaded flow for linear resin transfer molding injections, Polymer Composites, 42(8) (2021), 3980–3995.